Minimal phase-coupling model for intermittency in turbulent systems

José-Agustín Arguedas-Leiva [1] Enda Carroll [2] Luca Biferale,[3] Michael Wilczek [1,4,*] and Miguel D. Bustamante [2]

[1]*Max Planck Institute for Dynamics and Self-Organization, Am Faßberg 17, 37077 Göttingen, Germany*
[2]*School of Mathematics and Statistics, University College Dublin, Belfield, Dublin 4, Ireland*
[3]*Department Physics and Istituto Nazionale Fisica Nucleare (INFN), University of Rome Tor Vergata, Via Ricerca Scientifica 1, 00133 Rome, Italy*
[4]*Theoretical Physics I, University of Bayreuth, Universitätsstraße 30, 95447 Bayreuth, Germany*

Turbulent systems exhibit a remarkable multiscale complexity, in which spatial structures induce scale-dependent statistics with strong departures from Gaussianity. In Fourier space, this is reflected by pronounced phase synchronization. A quantitative relation between real-space structure, statistics, and phase synchronization is currently missing. Here, we address this problem in the framework of a minimal deterministic phase-coupling model, which enables a detailed investigation by means of dynamical systems theory and multiscale high-resolution simulations. We identify the spectral power law steepness, which controls the phase coupling, as the control parameter for tuning the non-Gaussian properties of the system. Whereas both very steep and very shallow spectra exhibit close-to-Gaussian statistics, the strongest departures are observed for intermediate slopes comparable with the ones in hydrodynamic and Burgers turbulence. We show that the non-Gaussian regime of the model coincides with a collapse of the dynamical system to a lower-dimensional attractor and the emergence of phase synchronization, thereby establishing a dynamical-systems perspective on turbulent intermittency.

I. INTRODUCTION

Turbulence is a prototypical nonequilibrium phenomenon with a large number of strongly interacting degrees of freedom [1–6], exhibiting strong departures from Gaussianity on the smallest spatial scales. In real space, non-Gaussian fluctuations can be related to coherent, intense, and rare events in the velocity gradients—a phenomenon also dubbed as *intermittency* [7,8]. Intermittency can also be studied from the complementary perspective of Fourier space. While Gaussian random fields feature completely uncorrelated phases, phase correlations can give rise to complex scale-dependent properties, as the ones developed in the presence of coherent shocks.

Elucidating these connections is important for both fundamental and applied aspects. We are currently missing a clear identification of which dynamical degrees of freedom lead to such bursting and quiescent chaotic alternations of temporal and spatial flow realizations. As a result, we lack optimal protocols to avoid disrupting fluctuations in engineering turbulence [9,10], to predict extreme events in geophysical flows [11,12], and to control existence and uniqueness of the partial

differential equation (PDE) solutions [13], just to cite a few open problems with multidisciplinary impacts. Studying these issues in fully developed three-dimensional turbulence is an extremely challenging task. The hope is to isolate the main aspects of this problem in simpler, more tractable models. One popular way is to lower the complexity by mode reduction, as in the case of subgrid-scale modeling [14,15], Fourier surgery [16,17], statistical closure [18], partial freezing of some spectral degrees of freedom [19,20], or asymptotic expansions [21,22]. All attempts have merits and deficiencies, the main common drawback being the compromised ability to describe simultaneously spatial and temporal fluctuations on a wide range of scales. Notably, only very few studies have addressed the connection between the emergence of coherent intermittent structures in real space and phase correlations, connecting the presence of bursts of spectral energy fluxes (and dissipation) with Fourier phase dynamics [23–27].

In this letter, we combine theory and simulations to provide a dynamical systems link between real-space intermittency and phase correlations in Fourier space. We do so by means of a minimal deterministic description of hydrodynamic turbulence derived from a PDE model, preserving the whole richness of multiscale spatial and temporal statistics. The model is formulated in terms of Fourier phases whose dynamical coupling resembles the one in Navier-Stokes turbulence: specifically, it is Burgers turbulence with the important distinction that the amplitudes are kept at fixed values such that only the phases evolve, obeying a deterministic system that supports a turbulent attractor. By changing the energy spectrum slope, we can tune the coupling strength of the phases and study how the dynamics (intermittency) changes.

We find that the system transitions to non-Gaussian statistics as the spectrum is gradually steepened. For slopes beyond a certain value, the rare fluctuations become less extreme and return to near-Gaussian statistics. Strikingly, the strongest deviations occur in the intermediate range, within the range of values attained by turbulent systems. Within this range, the dimension of the strange attractor collapses to a minimum, indicating that non-Gaussian real-space statistics are related to the collapse of the dynamical system onto a lower-dimensional manifold.

Our analysis sheds light on the emergence of coherent structures and the associated phase synchronization phenomena [28], establishing connections between the statistical theory of nonequilibrium systems and dynamical systems theory.

II. THE MODEL

As a starting point, let us consider the one-dimensional Burgers equation:

$$\partial_t u(t, x) + u(t, x)\partial_x u(t, x) = \nu \partial_x^2 u(t, x). \tag{1}$$

This simple prototypical PDE is reminiscent of the Navier-Stokes equations, known to develop multiscale bifractal scaling properties, shocks, non-Gaussian statistics, and many other nontrivial statistical features [29–38].

We consider a one-dimensional field $u(t, x)$ on a 2π-periodic domain with Fourier decomposition:

$$u(t, x) = \sum_{k \in \mathbb{Z}} a_k(t) \exp(i[\varphi_k(t) + kx]). \tag{2}$$

By inserting Eq. (2) into Eq. (1), we obtain the evolution for the amplitudes and the phases:

$$a_k \frac{d\varphi_k}{dt} = -\frac{k}{2}\sum_{p \in \mathbb{Z}} a_p\, a_{k-p}\, \cos(\varphi_p + \varphi_{k-p} - \varphi_k), \tag{3}$$

$$\frac{da_k}{dt} = \frac{k}{2}\sum_{p \in \mathbb{Z}} a_p\, a_{k-p}\, \sin(\varphi_p + \varphi_{k-p} - \varphi_k) - \nu k^2 a_k. \tag{4}$$

This infinite set of coupled ordinary differential equations describes the full Burgers dynamics of the Fourier phases and amplitudes.

Recently, we showed that the dynamics of the Fourier phases $\varphi_k(t)$ determine to a great extent the shock dynamics and the associated non-Gaussian statistics when the amplitudes follow a Burgers-like scaling [27]. To establish a deeper dynamical systems understanding of the role of Fourier phases in turbulence, we now follow a different approach, by introducing a minimal deterministic model enjoying a turbulent attractor. Take Eq. (3) as a starting point and set the amplitudes to prescribed constants:

$$a_k = |k|^{-\alpha}, \quad |k| > k_0, \quad a_k = 0, \quad |k| \leqslant k_0, \tag{5}$$

where the steepness α is our new *continuous control parameter*, and $k_0 > 0$ is a large-scale cutoff leading to a finite integral length scale, which destabilizes a single-shocklike fixed point, allowing thus for a turbulent attractor.
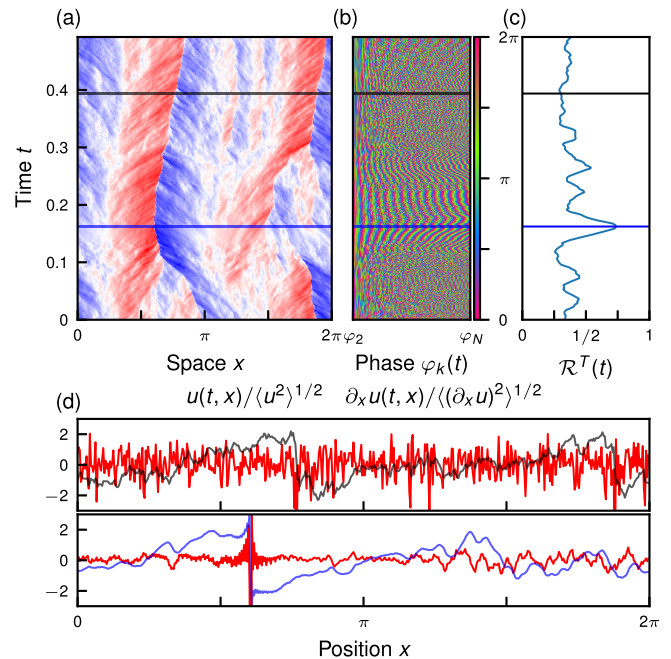

FIG. 1. Numerical simulations of Eq. (6) with $k_0 = 1$ and $N = 2^9$, with a Burgers-like steepness parameter $\alpha = 1$. (a) Plot of the real-space field $u(t, x)$ displaying a shock near $x = \pi/2$ at the time indicated by the blue line. The field $u(t, x)$ is obtained by solving the phase dynamics in Eq. (6) and inserting the time-evolving phases into Eq. (2) for prescribed amplitudes a_k. (b) Plot of individual phases $\varphi_2, \ldots \varphi_N$. The gray line marks an instance of a relatively disordered regime, while the blue line marks a relatively synchronized regime. (c) Time-dependent order parameter $\mathcal{R}^T(\alpha, t)$, cf. Eq. (10), for the synchronization of the system (here with $T = 0.0244$). The peak corresponds to a synchronization event related to a real-space shock. (d) Snapshots of the real-space field $u(t, x)$ in the disordered (top, gray) and synchronized (bottom, blue) regimes. Red curves show the gradient $\partial_x u(t, x)$ to illustrate the difference between the two regimes.

The phase dynamics is obtained from Eq. (3) which becomes a system of coupled oscillators φ_k satisfying

$$\frac{d\varphi_k}{dt} = \sum_{p \in \mathbb{Z}} \omega_{k,p}\, \cos(\varphi_p + \varphi_{k-p} - \varphi_k), \quad |k| > k_0, \tag{6}$$

with coefficients $\omega_{k,p} = -k\,|p(k-p)|^{-\alpha}\,|k|^\alpha$ when $|k - p|, |p| > k_0$ ($\omega_{k,p} = 0$ otherwise), and with $\varphi_{-k} = -\varphi_k$ (reality condition). Compared with Eq. (3), we have rescaled time in Eq. (6) to absorb the factor $\frac{1}{2}$. The triadic interaction term couples the phases with wave numbers k, p, and $k - p$, via the so-called triad phase $\varphi_{p,k-p}^k := \varphi_p + \varphi_{k-p} - \varphi_k$. It is important to note that this phase-only model does not need an energy input/output mechanism, as constant energy is maintained by the constant amplitudes. Furthermore, it is formally fully time reversible under the symmetry $t \to -t; \varphi_k \to \varphi_k + \pi$. However, it will not come as a surprise that, like in a formally reversible version of the Navier-Stokes equations [39–42], the chaotic dynamics spontaneously break the time symmetry, leading to a non-Gaussian and skewed velocity increment probability density function (PDF).
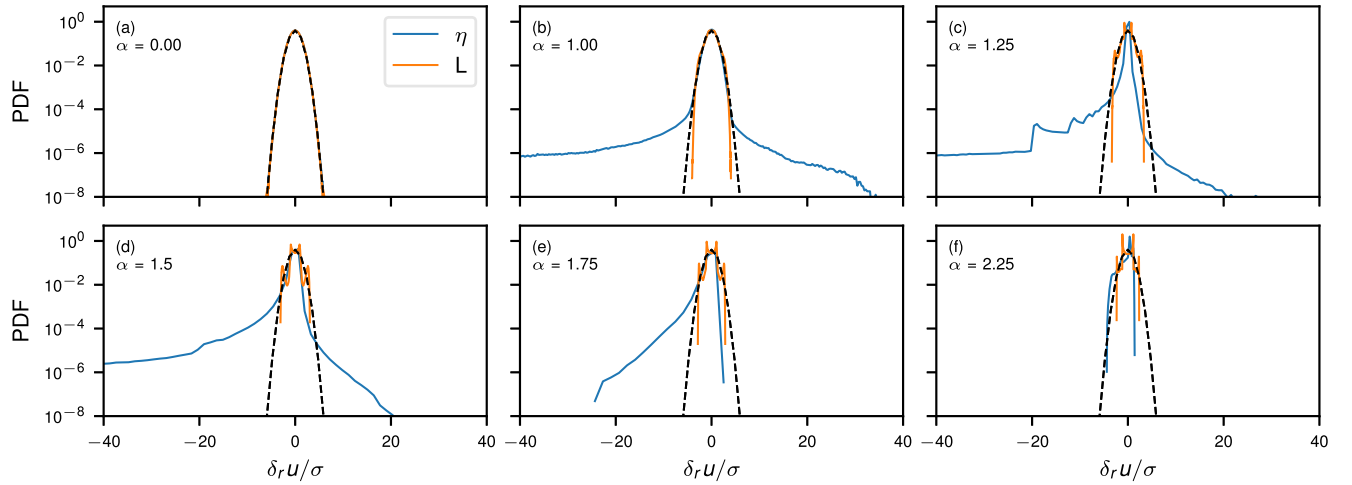
FIG. 2. (a)–(f) Standardized probability density functions (PDFs) of $\delta_r u$ calculated at the smallest η and largest increments L. (a) For flat Fourier amplitudes $\alpha = 0$, the velocity field is Gaussian across all scales. (b)–(e) Increasing α leads to heavy tails at small scales. (f) For a steep enough spectrum, the velocity field is dominated by the first few modes leading to PDFs without heavy tails. Data for $N = 2^{15}$ and $k_0 = 1$.

To study the model numerically, we further introduce a discretization with grid spacing $\Delta x = \pi/N$, effectively setting $a_k = 0$, $|k| > N$. The reality condition $\varphi_{-k} = -\varphi_k$ leaves us with a set of phases evolving on modes $k_0 < k \leqslant N$. We set $k_0 = 1$ so $a_1 = a_{-1} = 0$, and thus, the evolving variables are $\varphi_2, \ldots, \varphi_N$.

Note that the energy spectrum of the field is fixed and perfectly self-similar: $E_k \sim a_k^2$, with a power law decay of $E_k \propto k^{-2\alpha}$. The observed original Burgers case, where quasidiscontinuities (shocks) dominate the high-order statistics, corresponds to $\alpha = 1$.

III. NUMERICAL RESULTS ON REAL-SPACE AND PHASE DYNAMICS AND STATISTICS

We integrate numerically Eq. (6) with a fourth-order Runge-Kutta method starting from uniformly random initial conditions. The nonlinear term can be written as a convolution, which we efficiently evaluate with a pseudospectral method.

Figure 1 illustrates the dynamics of our model, for the choice of steepness $\alpha = 1$ (Burgers case), revealing insights into the relation between non-Gaussianity of the real-space statistics and Fourier phase synchronization. Panel (a) is a space-time plot of the velocity field from this minimal model, showing that shocks are the dominant structure. As time evolves, shocks steadily merge and separate. Occasionally, they merge into one dominating shock (horizontal blue line). Panel (b) shows a time series of the individual Fourier phases of the model. It shows that the presence of this dominating shock corresponds to highly ordered patterns in the phase plot. Away from these events, the system is dominated by smaller shocks, and we observe a low coherence (gray line). To quantify this, panel (c) shows the time-dependent average phase synchronization in Eq. (10), which reveals the synchronization of the oscillator system locally in time. The time of the highest synchronization corresponds to the dominating shock in real space. Panel (d) shows that the presence of the

dominating shock (blue line) yields extreme events in the gradient field characterizing the small scales of the velocity field.

By changing the free parameter α in Eq. (6), we control the multiscale coupling among the phases and the hierarchical organization of typical time scales. In a *local* approximation, i.e., supposing the dynamics at wave number k is mainly driven by triads around the same wave number $|k| \sim |k - p| \sim |p|$, we can estimate the scale-dependent eddy-turnover time as $\tau_k \sim |k|^{\alpha-1}$, indicating that, within this approximation, we reach a regime where small scales are faster than the large scales if $\alpha < 1$ (and slower if $\alpha > 1$). The local-triad approximation is expected to be valid in the range $0.5 < \alpha < 1.5$ [43], where the Fourier transform connecting the spectrum and the two-point velocity correlation function does not diverge, neither in the ultraviolet nor in the infrared. As a result, we expect that, in the above range and around $\alpha = 1$, a nontrivial balancing between spatial and temporal fluctuations will set in.

In Fig. 2, we indeed observe that our model has nontrivial scale- and steepness-dependent statistics. Here, we show the PDFs of the velocity increments $\delta_r u = u(x + r) - u(x)$ for two different scales, $r = L := \pi$ and $r = \eta := \pi/N$, denoting the largest and smallest distances in the periodic domain, respectively. Real-space statistics are obtained by inserting the phase dynamics into Eq. (2).

For completely uniform amplitudes (steepness $\alpha = 0$), the phases evolve under an all-to-all coupling with equal strength. Note that this choice of spectral amplitudes corresponds to a delta-correlated field in real space. In this case, all phases become dynamically uniformly distributed and uncorrelated, leading to a Gaussian velocity field at all scales [Fig. 2(a)]. In contrast, for steepness values within the range [0.5, 1.5], where the local-triad approximation is expected to be valid, heavy tails are observed in the velocity increment PDF at small scales [Figs. 2(b)–2(d)]. For the smallest increment, the negative PDF tails are much heavier than the positive tails, and both are much heavier than Gaussian. Heuristically (to be quantified later), this is the result of phase synchronization
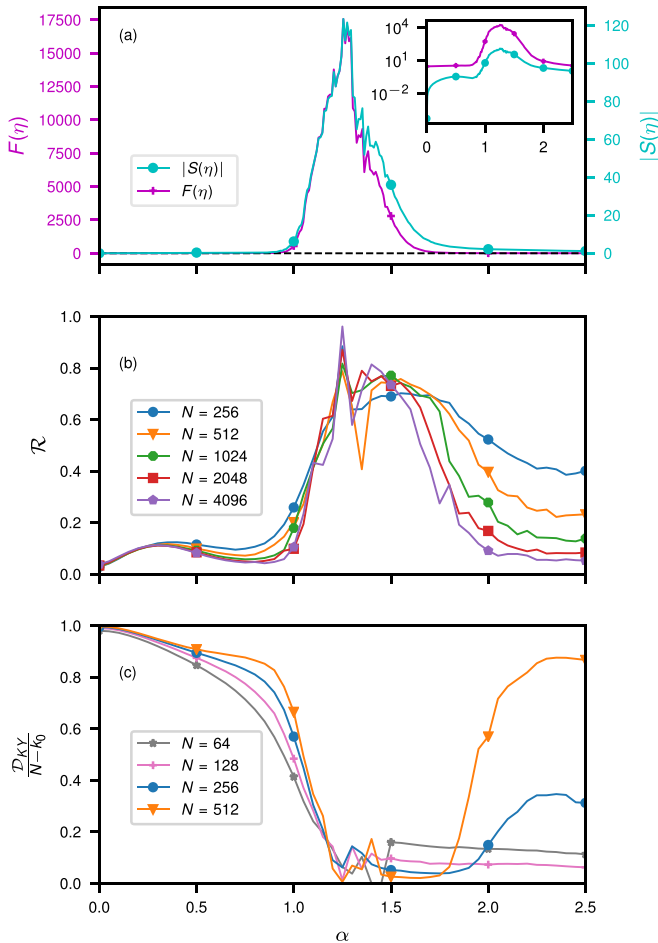
FIG. 3. (a) Absolute value of the skewness $|S(\eta)|$ and the flatness $F(\eta)$ for the smallest increment η as a function of α (inset: same figure on log-lin scales, $N = 2^{15}$). (b) Time- and scale-averaged phase synchronization $\mathcal{R}(\alpha)$ as a function of α for various system sizes. (c) Ratio between the Kaplan-Yorke (KY) dimension $\mathcal{D}_{KY}$ and $N - k_0$ as a function of α for various system sizes.

leading to shocks (antishocks), i.e., extreme negative (positive) gradients.

The presence of extreme events is maximal at $\alpha \sim 1.25$, as evidenced in Fig. 2(c). For higher values of α, the PDF tails slowly regularize. In this limit, the large-scale modes dominate the real-space velocity field, leading to a dominant sinusoidal mode with superimposed smaller fluctuations. As a consequence, the large α limit shows close-to-Gaussian statistics throughout.

To quantify the steepness-dependent departure of the small scales from Gaussianity, we measure the skewness and flatness:

$$S(r) = \frac{\langle (\delta_r u)^3 \rangle}{\langle (\delta_r u)^2 \rangle^{3/2}}, \quad F(r) = \frac{\langle (\delta_r u)^4 \rangle}{\langle (\delta_r u)^2 \rangle^2}. \quad (7)$$

Due to our frozen-amplitude condition, the denominators of both quantities do not fluctuate. Figure 3(a) shows a clear transition at $\alpha \sim 1.0$. The peaks of skewness and flatness at $\alpha \sim 1.25$ correspond to the presence of extremely intense negative gradients seen in Fig. 2(c).

As the steepness is increased further, the phases evolve under a nonlocal and nontrivial triad coupling. This gives rise to synchronization events, which underlie the steepness-dependent transition observed in the real-space statistics. Note, however, that when the steepness is too large, the timescales from the triad coupling can get too separated, as the coefficients $\omega_{k,p}$ in Eq. (6) become too small when $|p|$ and $|k - p|$ are large. Thus, we expect to see synchronization over a finite range of steepness values only. In the next sections, we will quantify the dependence on the α parameter of synchronization and of the structure of the associated chaotic attractors.

IV. SYNCHRONIZATION

We quantify the behavior of triad phases across a range of scales for Eq. (6) by defining the scale-dependent collective phase θ_k:

$$\exp(i\theta_k) = \frac{\sum_{p \in \mathbb{Z}} a_p a_{k-p} \exp[i(\varphi_p + \varphi_{k-p} - \varphi_k)]}{\left| \sum_{p \in \mathbb{Z}} a_p a_{k-p} \exp[i(\varphi_p + \varphi_{k-p} - \varphi_k)] \right|}. \quad (8)$$

This collective phase is dynamically relevant as the right-hand side of Eq. (6) is proportional to $\cos \theta_k$. The fluctuations of θ_k over time serve as a measure of the triad phase coherence across scales. Thus, averaging over a causal time window T from $t - T$ to t, we get the following scale-dependent Kuramoto order parameter:

$$R_k^T(t) \exp\left[i\Theta_k^T(t)\right] = \langle \exp\left[i\theta_k(t)\right] \rangle_T. \quad (9)$$

As usual, we have $0 \leqslant R_k^T \leqslant 1$, and phase synchronization is indicated by R_k^T values close to 1. Averaging additionally over the spatial scales, we define the average phase synchronization by

$$\mathcal{R}^T(\alpha, t) = \frac{1}{N - k_0} \sum_{k=k_0+1}^{N} R_k^T(t), \quad (10)$$

which measures how the phase synchronization changes as a function of the spectral slope. As discussed earlier, we evaluated the time-dependent average phase synchronization $\mathcal{R}^T$ in Fig. 1(c) to establish the correspondence between real-space structures and phase synchronization. For very large T, we obtain the time- and scale-averaged phase synchronization $\mathcal{R}(\alpha) = \lim_{T \to \infty} \mathcal{R}^T(\alpha, t)$.

Figure 3(b) shows the average phase synchronization $\mathcal{R}(\alpha)$ as a function of α for various system sizes N. The relatively high synchronization seen for small N at $\alpha > 2.0$ decreases as N is increased. This is due to the addition of faster and noisier oscillators to the system causing a convergence toward a pronounced peak for $\alpha \in [1.0, 2.0]$, indicating high phase synchronization for this interval for large N. The synchronization peak is remarkably coincidental with the flatness and skewness peaks shown in Fig. 3(a), providing quantitative evidence in support of the relation between synchronization (a dynamical-system measure) and intermittency (a real-space measure).

V. CHAOS CHARACTERIZATION

As an additional characterization of the dynamical system, we estimate the properties of the underlying strange attractor as a function of α and for $N = 64$, 128, 256, and 512 by examining the Lyapunov exponents (LEs) [44].

For reasons of numerical complexity, we cannot reach the same resolution we used for the statistical characterization of intermittency and synchronization; however, as we will see below, the $N = 512$ case shows strong indications of convergence to the large-N limit.

Using the LEs, we can calculate the dimension of the attractor via the Kaplan-Yorke (KY) approximation [45,46]. Given the ordered LEs $\lambda_1 \geqslant \lambda_2 \geqslant \cdots \geqslant \lambda_{N-k_0}$, the KY dimension is defined as

$$\mathcal{D}_{\mathrm{KY}} = J + \frac{\sum_{j=1}^{J} \lambda_j}{|\lambda_{J+1}|}, \tag{11}$$

where the conditions $\sum_{j=1}^{J} \lambda_j \geqslant 0$ and $\sum_{j=1}^{J+1} \lambda_j < 0$ define the index J. The KY dimension gives a measure of the effective degrees of freedom of the systems. Figure 3(c) shows a plot of the ratio between the $\mathcal{D}_{\mathrm{KY}}$ and the number of available degrees of freedom as a function of α and for several values of N. It is evident that, as N grows, a clear pattern emerges, whereby $\mathcal{D}_{\mathrm{KY}}$ greatly diminishes for values of α inside the interval [1.0, 2.0], a behavior that coincides, on the one hand, with the departure from Gaussianity observed in Fig. 3(a) and, on the other hand, with the increase in phase synchronization shown in Fig. 3(b).

VI. CONCLUSIONS

Our minimal model sheds light on the nature of coherent structures as low-dimensional objects, establishing a dynamical scenario where real-space intermittency and phase synchronization are accompanied by a reduction in the dimensions of the attractor.

In our model, coherent structures are controlled by Fourier phase dynamics only, as the energy spectrum is static and plays a background role. Our results open perspectives concerning the possibility to connect turbulence intermittency with dynamical system tools based on phase synchronization and chimera states [47].

On the quantitative side, our results provide insight into the solution to the full inviscid Burgers equation, where all amplitudes are allowed to evolve. There, for generic initial conditions, a finite-time singularity develops characterized by phase synchronization and a power law spectrum with steepness $1.33 \leqslant \alpha \leqslant 1.50$ [48,49]. We have checked that this behavior is robust, occurring even under the constraint $a_{k_0} = 0$ for $k_0 = 1$. Because in the full equations the spectrum evolves slowly, it is natural to expect that, in our frozen-spectrum constrained model, the phases must show high correlation in the same range of imposed slopes.

A natural extension of this work would be an investigation of the phase-only three-dimensional Navier-Stokes dynamics by fixing the amplitudes of all Fourier modes, including comparisons with Navier-Stokes equations with a fixed spectrum, either for all wave numbers or for a subset of them [19,20]. Results in this direction would help to shed additional light on the origin of extreme events and small-scale intermittency.

[1] U. Frisch, *Turbulence: The Legacy of A. N. Kolmogorov* (Cambridge University Press, Cambridge, 1995).

[2] K. R. Sreenivasan, Fluid turbulence, Rev. Mod. Phys. **71**, S383 (1999).

[3] S. B. Pope, *Turbulent Flows* (Cambridge University Press, Cambridge, 2000).

[4] P. A. Davidson, *Turbulence: An Introduction for Scientists and Engineers* (Oxford University Press, Oxford, 2015).

[5] A. Alexakis and L. Biferale, Cascades and transitions in turbulent flows, Phys. Rep. **767-769**, 1 (2018).

[6] D. Biskamp, *Magnetohydrodynamic Turbulence* (Cambridge University Press, Cambridge, 2003).

[7] G. Parisi and U. Frisch, A multifractal model of intermittency, in *Turbulence and Predictability in Geophysical Fluid Dynamics and Climate Dynamics* (North-Holland, Amsterdam, 1985), pp. 84–88.

[8] R. H. Kraichnan, Models of Intermittency in Hydrodynamic Turbulence, Phys. Rev. Lett. **65**, 575 (1990).

[9] J. Jiménez, Cascades in wall-bounded turbulence, Annu. Rev. Fluid Mech. **44**, 27 (2012).

[10] T. Duriez, S. L. Brunton, and B. R. Noack, *Machine Learning Control-Taming Nonlinear Dynamics and Turbulence* (Springer, Cham, 2017).

[11] F. Ragone, J. Wouters, and F. Bouchet, Computation of extreme heat waves in climate models using a large deviation algorithm, Proc. Natl. Acad. Sci. USA **115**, 24 (2018).

[12] L. Biferale, F. Bonaccorso, I. M. Mazzitelli, M. A. T. van Hinsberg, A. S. Lanotte, S. Musacchio, P. Perlekar, and F. Toschi, Coherent Structures and Extreme Events in Rotating Multiphase Turbulent Flows, Phys. Rev. X **6**, 041036 (2016).

[13] C. L. Fefferman, Existence and smoothness of the Navier-Stokes equation, in *The Millennium Prize Problems*, edited by J. Carlson, A. Jaffe, and A. Wiles (Clay Mathematics Institute, Cambridge, 2006), pp. 57–67.

[14] C. Meneveau and J. Katz, Scale-invariance and turbulence models for large-eddy simulation, Annu. Rev. Fluid Mech. **32**, 1 (2000).

[15] R. Stevens, M. Wilczek, and C. Meneveau, Large-eddy simulation study of the logarithmic law for second- and higher-order

moments in turbulent wall-bounded flow, J. Fluid Mech. **757**, 888 (2014).

[16] L. Biferale, Shell models of energy cascade in turbulence, Annu. Rev. Fluid Mech. **35**, 441 (2003).

[17] T. Bohr, M. H. Jensen, G. Paladin, and A. Vulpiani, *Dynamical Systems Approach to Turbulence* (Cambridge University Press, Cambridge, 2005).

[18] M. Lesieur, *Turbulence in Fluids: Stochastic and Numerical Modelling* (Springer, Dordrecht, 1990).

[19] Z.-S. She and E. Jackson, Constrained Euler System for Navier-Stokes Turbulence, Phys. Rev. Lett. **70**, 1255 (1993).

[20] L. Biferale, F. Bonaccorso, M. Buzzicotti, and K. P. Iyer, Self-Similar Subgrid-Scale Models for Inertial Range Turbulence and Accurate Measurements of Intermittency, Phys. Rev. Lett. **123**, 014503 (2019).

[21] V. E. Zakharov, V. S. L'vov, and G. Falkovich, *Kolmogorov Spectra of Turbulence I: Wave Turbulence* (Springer-Verlag, Berlin, Heidelberg, 1992).

[22] S. Nazarenko, *Wave Turbulence* (Springer-Verlag, Berlin, Heidelberg, 2011), Vol. 825.

[23] M. Buzzicotti, B. P. Murray, L. Biferale, and M. D. Bustamante, Phase and precession evolution in the burgers equation, Eur. Phys. J. E **39**, 34 (2016).

[24] J. Reynolds-Barredo, D. Newman, P. Terry, and R. Sanchez, Fourier signature of filamentary vorticity structures in two-dimensional turbulence, EPL **115**, 34002 (2016).

[25] M. Wilczek, D. G. Vlaykov, and C. C. Lalescu, Emergence of non-Gaussianity in turbulence, in *Progress in Turbulence VII. Springer Proceedings in Physics*, edited by R. Örlü, A. Talamelli, M. Oberlack, and J. Peinke (Springer, Cham, 2017), Vol. 196.

[26] J.-A. Arguedas-Leiva, *Phase Coherence and Intermittency of a Turbulent Field Based on a System of Coupled Oscillators*, Master's thesis, Georg-August-Universität, Göttingen, 2017.

[27] B. P. Murray and M. D. Bustamante, Energy flux enhancement, intermittency and turbulence via Fourier triad phase dynamics in the 1-D Burgers equation, J. Fluid Mech. **850**, 624 (2018).

[28] In this letter, *synchronization* is understood as a transient state whereby the phases of the Fourier modes over an extended range of spatial scales evolve following similar patterns, showing strong correlations during finite time intervals. This is like the definition used in classical phase models [50,51], although, in this letter, we study synchronization in a Fourier phase model based on a system with quadratic nonlinearity.

[29] O. Zikanov, A. Thess, and R. Grauer, Statistics of turbulence in a generalized random-force-driven Burgers equation, Phys. Fluids **9**, 1362 (1997).

[30] E. Balkovsky, G. Falkovich, I. Kolokolov, and V. Lebedev, Intermittency of Burgers' Turbulence, Phys. Rev. Lett. **78**, 1452 (1997).

[31] J. Bec and K. Khanin, Burgers turbulence, Phys. Rep. **447**, 1 (2007).

[32] G. Da Prato, A. Debussche, and R. Temam, Stochastic Burgers' equation, NoDEA **1**, 389 (1994).

[33] A. Chekhlov and V. Yakhot, Kolmogorov turbulence in a random-force-driven Burgers equation, Phys. Rev. E **51**, R2739(R) (1995).

[34] G. L. Eyink and T. D. Drivas, Spontaneous stochasticity and anomalous dissipation for Burgers equation, J. Stat. Phys. **158**, 386 (2015).

[35] Z.-S. She, E. Aurell, and U. Frisch, The inviscid Burgers equation with initial data of Brownian type, Commun. Math. Phys. **148**, 623 (1992).

[36] J.-P. Bouchaud, M. Mézard, and G. Parisi, Scaling and intermittency in Burgers turbulence, Phys. Rev. E **52**, 3656 (1995).

[37] Weinan E, K. Khanin, A. Mazel, and Y. Sinai, Invariant measures for Burgers equation with stochastic forcing, Ann. Math. **151**, 877 (2000).

[38] M. Buzzicotti, L. Biferale, U. Frisch, and S. S. Ray, Intermittency in fractal Fourier hydrodynamics: lessons from the Burgers equation, Phys. Rev. E **93**, 033109 (2016).

[39] G. Gallavotti, Nonequilibrium in statistical and fluid mechanics. Ensembles and their equivalence. Entropy driven intermittency, J. Math. Phys. **41**, 4061 (2000).

[40] G. Gallavotti, Entropy, thermostats and chaotic hypothesis, Chaos **16**, 043114 (2006).

[41] L. Biferale, M. Cencini, M. De Pietro, G. Gallavotti, and V. Lucarini, Equivalence of non-equilibrium ensembles in turbulence models, Phys. Rev. E **98**, 012202 (2018).

[42] V. Shukla, B. Dubrulle, S. Nazarenko, G. Krstulovic, and S. Thalabard, Phase transition in time-reversible Navier-Stokes equations, Phys. Rev. E **100**, 043104 (2019).

[43] H. Rose and P. Sulem, Fully developed turbulence and statistical mechanics, J. Phys. **39**, 441 (1978).

[44] F. Ginelli, P. Poggi, A. Turchi, H. Chaté, R. Livi, and A. Politi, Characterizing Dynamics with Covariant Lyapunov Vectors, Phys. Rev. Lett. **99**, 130601 (2007).

[45] J. L. Kaplan and J. A. Yorke, Chaotic behavior of multi-dimensional difference equations, in *Functional Differential Equations and Approximation of Fixed Points, Lecture Notes in Mathematics*, edited by H. O. Peitgen and H. O. Walther (Springer, Berlin, Heidelberg, 1979), pp. 204–227.

[46] P. Frederickson, J. L. Kaplan, E. D. Yorke, and J. A. Yorke, The Liapunov dimension of strange attractors, J. Diff. Equ. **49**, 185 (1983).

[47] I. Shepelev, G. Strelkova, and V. Anishchenko, Chimera states and intermittency in an ensemble of nonlocally coupled Lorenz systems, Chaos **28**, 063119 (2018).

[48] C. Sulem, P.-L. Sulem, and H. Frisch, Tracing complex singularities with spectral methods, J. Comput. Phys. **50**, 138 (1983).

[49] M. D. Bustamante and M. Brachet, Interplay between the Beale-Kato-Majda theorem and the analyticity-strip method to investigate numerically the incompressible Euler singularity problem, Phys. Rev. E **86**, 066302 (2012).

[50] M. G. Rosenblum, A. S. Pikovsky, and J. Kurths, Phase Synchronization of Chaotic Oscillators, Phys. Rev. Lett. **76**, 1804 (1996).

[51] S. Boccaletti, J. Kurths, G. Osipov, D. Valladares, and C. Zhou, The synchronization of chaotic systems, Phys. Rep. **366**, 1 (2002).